Available online at www.sciencedirect.com

ScienceDirect

Journal of Hazardous Materials 157 (2008) 367–373

Journal of Hazardous Materials

www.elsevier.com/locate/jhazmat

Hydrodynamic characteristics of airlift nitrifying reactor using carrier-induced granular sludge

Ren-Cun Jin [a,b], Ping Zheng [a,*], Qaisar Mahmood [a], Lei Zhang [a]

[a] *Department of Environmental Engineering, Zhejiang University, Hangzhou 310029, PR China*
[b] *Department of Environmental Science, Hangzhou Normal University, Hangzhou 310036, PR China*

Received 21 June 2007; received in revised form 28 December 2007; accepted 3 January 2008
Available online 8 January 2008

Abstract

Since nitrification is the rate-limiting step in the biological nitrogen removal from wastewater, many studies have been conducted on the immobilization of nitrifying bacteria. A laboratory-scale investigation was carried out to scrutinize the effectiveness of activated carbon carrier addition for granulation of nitrifying sludge in a continuous-flow airlift bioreactor and to study the hydrodynamics of the reactor with carrier-induced granules. The results showed that the granular sludge began to appear and matured 60 and 108 days, respectively, after addition of carriers, while no granule was observed in the absence of carriers in the control test. The mature granules had a diameter of 0.5–5 mm (1.6 mm in average), settling velocity 22.3–55.8 $\mathrm{m\,h^{-1}}$ and specific gravity of 1.086. The relationship between the two important hydrodynamic coefficients, i.e. gas holdup and liquid circulation velocity, and the superficial gas velocity were established by a simple model and were confirmed experimentally. The model also could predict the critical superficial gas velocity for liquid circulation and that for granules circulation, with respective values of 1.017 and 2.662 $\mathrm{cm\,min^{-1}}$, accurately.

Keywords: Airlift reactor; Granular sludge; Nitrification; Hydrodynamic characteristic; Activated carbon

---

1. Introduction

Nitrogenous compounds like ammonium are prevalent in many wastewaters and need to be removed to prevent oxygen depletion and eutrophication of surface waters. Biological nitrogen removal from wastewater using nitrification–denitrification is a well-known and cost-effective treatment process [1,2]. Because of their extremely low growth rate, it is generally accepted that retaining a large number of nitrifying bacteria within the reactor is difficult to achieve, thereby making the nitrification a rate-limiting step in the entire nitrogen removal process [3,4].

Much work has been conducted on the development of physical or ecological methods of immobilizing nitrifying bacteria including cell-entrapping and cell-attaching techniques [5–7]. However, the immobilized cells created by gel entrapping techniques are easy to be suffered from mass transfer resistance [5]. Previous researches also demonstrated that it takes a long time to construct a nitrifying biofilm on the surface of carrier materials, particularly when the wastewater contains few organic compounds [8]. Moreover, the matrices and carriers used for cell immobilization inevitably occupy significant space in the reactor, limiting cell density. To avoid these problems, granular sludge was generated to enhance cell retention and biomass concentration simultaneously.

Sludge granulation has been intensively studied in anaerobic systems such as upflow anaerobic sludge blanket (UASB) [9,10] and in aerobic systems [11–13], but these reports have mostly focused on organic pollutant removal and the aerobic granular reactor used in these tests were mainly sequencing batch reactors (SBR) [11,12,14–17]. Until now, fewer attempts have been made to culture aerobic granular sludge in a continuous-flow system.

Three-phase airlift reactors (ALR) are being applied frequently in chemical, biotechnological and environmental processes as simple and effective gas–liquid–solid phase contactors. ALR offers advantages over traditional three-phase contactors, namely, a lower gas requirement for complete suspension of the solid, elimination of dead volumes, rapid mixing

---

[*] Corresponding author. Fax: +86 571 86971709.
E-mail address: pzheng@zju.edu.cn (P. Zheng).

0304-3894/$ – see front matter © 2008 Elsevier B.V. All rights reserved.
doi:10.1016/j.jhazmat.2008.01.003

and absence of external recirculation systems [18]. Their construction is simple but characterization of their hydrodynamic is a difficult task due to the presence of three phases. The four main hydrodynamic parameters in the description of ALR flow behavior are gas holdup, liquid circulation velocity, critical superficial air velocity for liquid circulation and that for solid circulation [18].

Until now, no attempt has been made to model the hydrodynamics of airlift reactor containing granular sludge. In the present study, we demonstrated an effective way to develop nitrifying granular sludge. A novel approach involving addition of support carrier, granular activated carbon, into the internal -loop airlift reactor allowed rapid and efficient granular sludge formation. The other aim of the present work was to propose a simple model that could simulate the liquid circulation and the gas holdup, and could predict the critical superficial air velocity for liquid circulation and that for solid circulation.

2. Hydrodynamic model

Once designed and constructed, ALR only has operational parameter gas flow rate to control the performance. Therein, the gas holdup, liquid circulation velocity, critical aeration flux should be related to the gas flow rate or aeration flux in hydrodynamic model.

2.1. Gas holdup

In an ALR, the difference between density of mixed liquid, which was determined by gas holdup, in the riser and downcomer regions creates a driving force for liquid circulation. Thus, the gas holdup is one of the most important hydrodynamic parameters.

There are two main forces drawing bubbles in the riser: buoyancy and drag force. In steady state, the balance between them is expressed as the following equation:

$$F_\mathrm{f} = F_\mathrm{d} \tag{1}$$

where the F_f = buoyancy and F_d = drag force. They can be obtained by [18]:

$$\begin{aligned} F_\mathrm{f} &= \frac{\pi}{6} d_\mathrm{b}^3 g(\rho_\mathrm{l} - \rho_\mathrm{g}) \\ F_\mathrm{d} &= \frac{1}{8} \pi C_\mathrm{D} V_\mathrm{gr}^2 \rho_\mathrm{l} d_\mathrm{b}^2 \end{aligned} \tag{2}$$

where d_b = average bubble diameter, ρ_l and ρ_g = density of liquid phase and gas phase, respectively, C_D = coefficient of drag force, and V_gr = linear velocity of gas in riser. According to Kolmogoroff's theory of isotropic turbulence, the average diameter of bubble can be expressed as [19,20]

$$d_\mathrm{b} = k \frac{\sigma^{0.6}}{(\rho_\mathrm{l} g U_\mathrm{gr}/(1 + A_\mathrm{d}/A_\mathrm{r}))^{0.4} \rho_\mathrm{l}^{0.2}} \varepsilon_\mathrm{g}^c \left(\frac{\mu_\mathrm{l}}{\mu_\mathrm{g}}\right)^{0.25} \tag{3}$$

where U_gr = superficial gas velocity in riser, ε_g = gas holdup in ALR, σ = surface tension, μ_l and μ_g = viscosity of liquid and air, respectively, A_r and A_d = cross-section area of riser and downcomer, respectively, and k and c are constants.

Combination Eq. (1)–(3) yields the gas holdup model

$$\begin{aligned} \varepsilon_\mathrm{g} &= a \left(1 + \frac{A_\mathrm{d}}{A_\mathrm{r}}\right)^{-0.4} U_\mathrm{gr}^b \\ a &= \left(\frac{0.75 C_\mathrm{D} \rho_\mathrm{L}^{1.4}}{k(g\sigma)^{0.6}(\rho_\mathrm{L} - \rho_\mathrm{g})(\mu_\mathrm{L}/\mu_\mathrm{g})^{0.25}}\right)^{1/c} \end{aligned} \tag{4}$$

where a and $b = 2.4/c$ are constants related to the constants in Eq. (1)–(3) and can be determined experimentally. For a given ALR, $A_\mathrm{d}/A_\mathrm{r}$ is fixed. So $a\,(1 + A_\mathrm{d}/A_\mathrm{r})^{-0.4}$ is a constant, expressed by β. Thus, gas holdup model can be simplified as

$$\varepsilon_\mathrm{g} = \beta U_\mathrm{gr}^b \tag{5}$$

It was established experimentally that there was a linear relation between gas holdup in riser and that in downcomer, which also can be modeled by applying fluid continuity theory [21,22]. In the ALR, the flow rate of the liquid in the riser is equal to that in the downcomer, and then we get the following equation:

$$U_\mathrm{lr} A_\mathrm{r} = U_\mathrm{ld} A_\mathrm{d} \tag{6}$$

where U_lr and U_ld = superficial liquid velocity in riser and downcomer, respectively and can be expressed by

$$\begin{aligned} U_\mathrm{lr} &= V_\mathrm{lr}(1 - \varepsilon_\mathrm{gr}) \\ U_\mathrm{ld} &= V_\mathrm{ld}(1 - \varepsilon_\mathrm{gd}) \end{aligned} \tag{7}$$

where V_lr and V_ld = linear liquid velocity in riser and downcomer, respectively; and ε_gr and ε_gd = gas holdup in riser and downcomer, respectively.

Then, the relationship between ε_gr and ε_gd can be deduced by Eq. (5)–(7) as

$$\varepsilon_\mathrm{gd} = \lambda \varepsilon_\mathrm{gr} - \gamma \tag{8}$$

where $\lambda = (V_\mathrm{lr}A_\mathrm{r})/(V_\mathrm{ld}A_\mathrm{d})$ and $\gamma = (V_\mathrm{lr}A_\mathrm{r})/(V_\mathrm{ld}A_\mathrm{d}) - 1$.

As shown in Eq. (8), the linear relationship between the gas holdup in riser and downcomer also can be obtained theoretically.

2.2. Liquid circulation velocity

One of the most significant characteristics of the ALR is the internal liquid circulation between the riser and the downcomer. Therefore, the liquid circulation is of prime importance for the design and scaleup of the ALR. There are various models on liquid circulation velocity [23–25]. Among them, the model given by Chisti et al. [26] is generally accepted.

$$U_\mathrm{lr} = K(1 - \varepsilon_\mathrm{gd})\sqrt{2gh_\mathrm{d}(\varepsilon_\mathrm{gr} - \varepsilon_\mathrm{gd})} \tag{9}$$

where h_d = height of gas–liquid dispersion and K is the constant depending on configurational parameter and resistance coefficient and can be determined experimentally.

Eq. (9) shows the relation between U_lr and the gas holdup. But, establishment of the relation between U_lr and U_gr also needs an explicit relationship between gas holdup and U_gr. Thus, it is

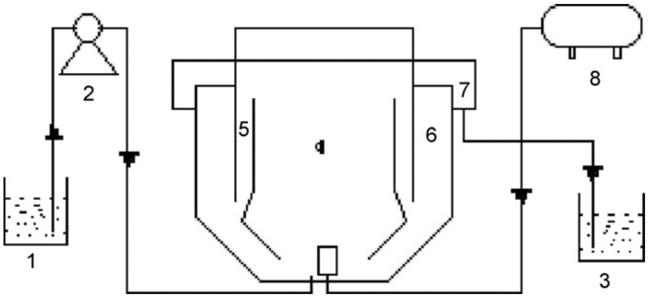

Fig. 1. Schematic illustration of the ALR used in the experiment: (1) influent tank, (2) peristaltic pump, (3) effluent tank, (4) riser, (5) downcomer, (6) settler, (7) overflow weir, and (8) air pump.

necessary to illustrate the relationship between ε_g, ε_{gr} and ε_{gd} as

$$\varepsilon_g(V_r + V_d) = \varepsilon_{gr} V_r + \varepsilon_{gd} V_d \tag{10}$$

where V_r and V_d = the volume of riser and downcomer, respectively.

Deduced from above, the model bridging U_{lr} to U_{gr} can be achieved by grouping Eqs. (5), (8)–(10).

3. Materials and methods

3.1. Airlift bioreactor

The schematic diagram of the ALR used in present study is shown in Fig. 1. This reactor was made of Perspex with a working volume of 10.4 L and height/diameter ratio of 1, consisting of four sections: riser, downcomer, gas separator, and settling section. The cross-sectional area of riser, downcomer and settling section were 153.9, 97.4 and 346.4 cm^2, respectively. The length of the riser was 15 cm. The carrier and the activated sludge were retained within ALR by the settling section equipped with an overflow weir. Aeration was carried out via a porous air diffuser ball. The reactor was operated at 30 ± 1 °C in a room equipped with thermostat.

3.2. Inoculum

Nitrifying sludge from a local municipal wastewater treatment plant (WWTP) was used as inoculum for the present study having initial volatile suspended solid (VSS) concentration of 5.8 g L^{-1}. The WWTP was operated under oxic/anoxic conditions.

3.3. Synthetic wastewater

The composition of synthetic wastewater is listed in Table 1. For alkalinity and carbon source supplement, the theoretical $NaHCO_3$ requirement for nitrification (7.1 g as $CaCO_3$ (g-NH_4-N)$^{-1}$) was added to the wastewater.

Table 1
Composition of synthetic ammonium-containing wastewater (in g L^{-1})

Compound	Concentration
KH_2PO_4	0.027
$MgSO_4 \cdot 7H_2O$	0.300
$CaCl_2$	0.136
$NaHCO_3$	Supplied as needed
$(NH_4)_2SO_4$	Supplied as needed
Trace elements I[a]	1.25 mL L^{-1}
Trace elements II[b]	1.25 mL L^{-1}

[a] Composition of trace elements I (g L^{-1}): EDTA, 5.00; $FeSO_4$, 5.00.

[b] Composition of trace elements II (g L^{-1}): EDTA, 15; $ZnSO_4 \cdot 7H_2O$, 0.43; $CoCl_2 \cdot 6H_2O$, 0.24; $MnCl_2 \cdot 4H_2O$, 0.99; $CuSO_4 \cdot 5H_2O$, 0.25; $Na_2MoO_4 \cdot 2H_2O$, 0.22; $NiCl_2 \cdot 6H_2O$, 0.19; $Na_2SeO_4 \cdot 10H_2O$, 0.21; $H_3BO_4 \cdot 7H_2O$, 0.014.

3.4. Carrier support

The matrices used as the carrier for the reactors was granular activated carbon (GAC). The characteristics of the GAC offered by the supplier (Cesun Activated Carbon, China) were as follows: size range, 0.5–0.8 mm; surface area, 1100–1250 m^2 g^{-1}; bulk density, 400–450 g L^{-1}; real density, 1340 g L^{-1}, water content ≤10% and ash content ≤3%.

3.5. Measurement

Ammonium, nitrite, nitrate, VSS and pH were determined using the standard methods [27]. The DO was measured by JPB-607 dissolved oxygen meter (Leici, China). The average diameter of granules was measured using an optical microscope (YS2-H, Nikon, China) as a circle-equivalent diameter of 100 granules randomly obtained from the airlift reactor. Measurements of specific gravity and settling velocity of granular sludge were carried out using the methods as described by Zheng et al. [17].

The volume expansion method was used to determine the gas holdup

$$\varepsilon = \frac{H_D - H_L}{H_D} \tag{11}$$

where H_D is the dispersion height and H_L is the liquid height.

The liquid circulation velocity was obtained using a fluoride trace method [19,28]. The method involves injecting a pulse of 10 mL of 5 g L^{-1} fluoride solution into the flowing liquid and plotting the time–concentration profile at two given points in the downcomer by means of two fluoride-probes connected to a computer. The linear liquid velocity in the downcomer V_{ld} was then obtained by the ratio of the distance between the two fluoride-probes and the differences in response times between the two sensors. The response time of fluoride-probe (less than 5 s) was lower than the measuring time; therefore, the influence of fluoride-probe dynamics on the measurement was neglected. Thus, the superficial gas velocity in riser can be worked out, by equation mentioned above.

4. Results and discussions

4.1. Performance of a carrier-free ALR (control experiment)

To evaluate the effect of activated carbon on granulation, a control run was conducted using an ALR operated under the

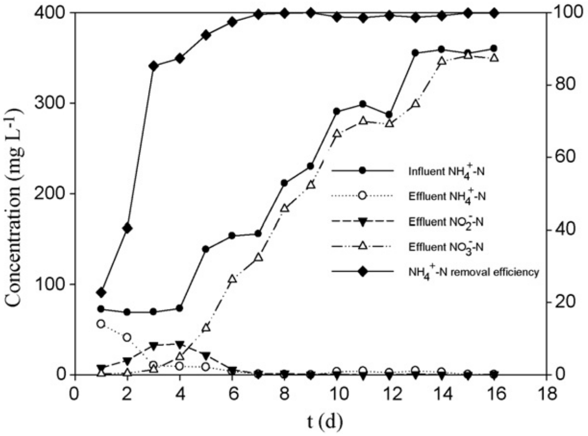

Fig. 2. Performance of the bioreactor during start-up.

same condition to those adopted for the ALR with carrier. No granules were noticed throughout the operation for more than 5 months.

4.2. Formation of nitrifying granules

As shown in Fig. 2, the reactor was started with 16 h HRT (flow rate at 15.6 L day^{-1}) and influent NH_4^+-N of 70 mg L^{-1}, corresponding to nitrogen loading rate (NLR) of 105 mg L^{-1} day^{-1}, at pH 7.2–7.5 and DO of 2.5–3.0 mg L^{-1}. Within 16 days, the influent NH_4^+-N was increased to 360 mg L^{-1}, with a concomitant increase in NLR to 540 mg L^{-1} day^{-1}.

After a satisfactory acclimation and culture of nitrifying bacteria, the reactor was operated for subsequent 26 days until a pseudo-steady-state was reached. The reactor worked stably at NLR of 540 mg L^{-1} day^{-1}, with an NH_4^+-N removal efficiency of 98%. To induce the granulation of nitrifying bacteria, 30 g granular activated carbon was added into the reactor on day 42. The formation of reddish and spherical nitrifying granules occurred within 2 months thereafter. Till day 150, the granular sludge prevailed in the ALR, with diameter of 0.5–5 mm (1.6 mm on average), settling velocity 22.3–55.8 m h^{-1} and specific gravity of 1.086. The photograph of floc-like nitrifying sludge on day 42 and nitrifying granule on day 150 are shown in Fig. 3.

It is assumed that the self-aggregation of microbes is characteristic to methane- and hydrogen-producing sludge [9,29,30] and even to denitrifying sludge [31]. Because, these bacteria are heterotrophic, they produce more extracellular polysaccharides than autotrophic bacteria [13]. Because of this property, heterotrophic bacteria are expected to be superior to autotrophic ones in terms of granulation. For this reason, there are only a few cases that aerobic autotrophic nitrifying bacteria form granular sludge as observed in this study [11,13]. Since no granule was observed in the absence of carriers in the control test, the method of adding activated carbon in present study may be the key to the granulation.

The role of carriers in granular sludge formation is still unclear, but it may be associated with the characteristics of biofilm formation on the carriers. It is suspected that the biofilm fraction detached from the carrier surface may serve as a seed to trigger the massive growth of granular sludge. Moreover, the enhanced granulation may be explained in part by the inert nuclei model or polymer-bonding model described by Liu et al. [9]. Further investigation is required to reveal its detailed mechanism.

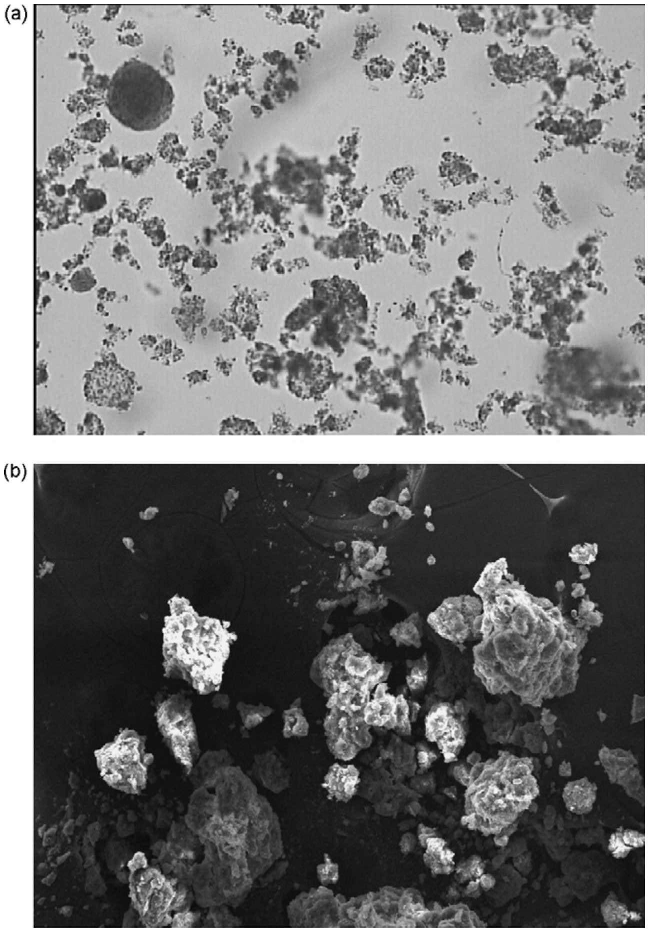

Fig. 3. The photograph of floc-like nitrifying sludge on: (a) day 42 (10 × 10); (b) day 150 (10 × 10).

4.3. Gas holdup

The results of hydrodynamic experiment are shown in Table 2. The Eq. (5) was made linear to gain the constants *b*

Table 2
Hydrodynamic parameters of airlift reactor with nitrifying granules

U_{gr} (cm min^{-1})	U_{lr} (cm s^{-1})	ε_{gr} (%)	ε_{gd} (%)	ε_g (%)
2.831	1.602	2.30	1.98	2.18
3.346	1.827	2.87	2.27	2.65
3.836	1.981	3.42	2.66	3.14
4.456	2.363	3.49	2.95	3.29
5.145	2.475	4.56	3.49	4.17
5.869	2.508	4.92	3.75	4.49
6.572	2.761	5.03	4.17	4.71
7.256	2.796	5.70	4.37	5.21

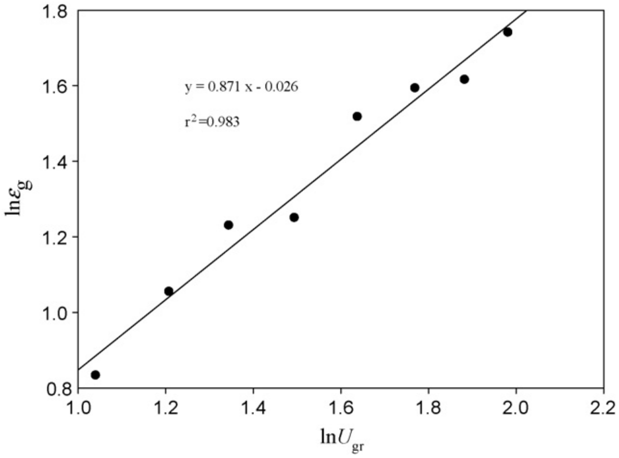

Fig. 4. Relationship between superficial gas velocity and total gas holdup.

and β:

$$\ln \varepsilon_g = b \ln U_{gr} + \ln \beta \tag{12}$$

Then, the linear regression analysis between $\ln \varepsilon_g$ and $\ln U_{gr}$ was conducted and the result is shown in Fig. 4. From the results, parameters $\beta = 0.942$ and $b = 0.871$ ($r^2 = 0.983$) were gained and the model for gas holdup could be expressed as Eq. (13).

$$\varepsilon_g = 0.942\, U_{gr}^{0.871} \tag{13}$$

The relationship between ε_{gd} and ε_{gr}, as shown in Fig. 5, was presented in Eq. (14) and the parameters λ and γ was 0.732 and 0.252 ($r^2 = 0.962$), respectively.

$$\varepsilon_{gd} = 0.732\, \varepsilon_{gr} + 0.252 \tag{14}$$

4.4. Liquid circulation velocity

Substituting b, β, λ and γ determined above into equation group composed by Eqs. (5), (8)–(10) can yield:

$$U_{lr} = K(13.8 - 0.127\, U_{gr}^{0.871})\sqrt{0.276\, U_{gr}^{0.871} - 0.28} \tag{15}$$

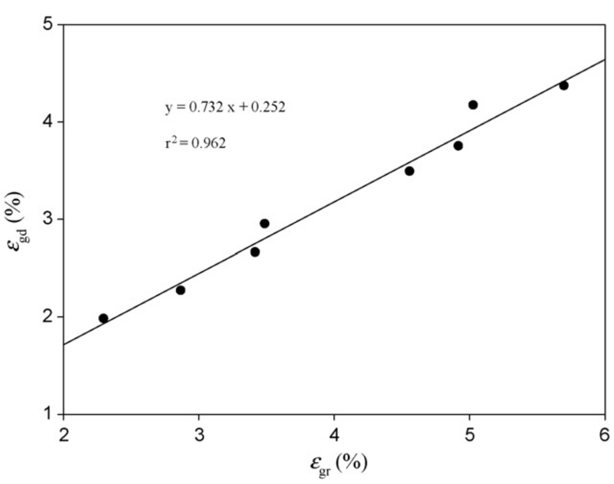

Fig. 5. Relationship between gas holdup in riser and that in downcomer.

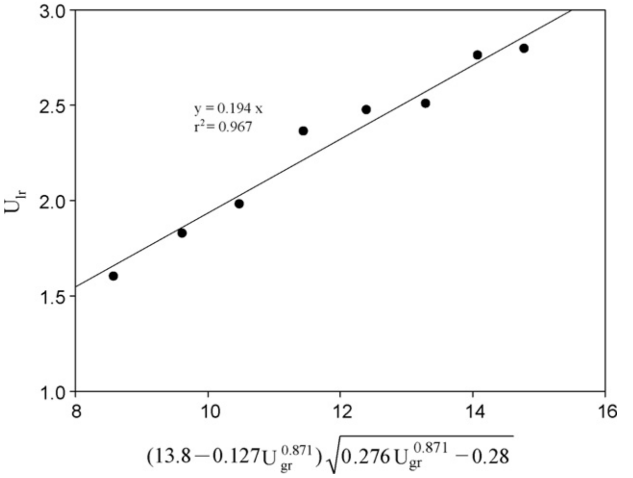

Fig. 6. Relationship between superficial velocity in riser and a function of superficial gas velocity.

As shown in Fig. 6, K was determined as 0.194 ($r^2 = 0.967$). Then, Eq. (15) can be written in the following form:

$$U_{lr} = (2.68 - 0.025\, U_{gr}^{0.871})\sqrt{0.276 U_{gr}^{0.871} - 0.28} \tag{16}$$

4.5. Critical superficial air velocity for liquid circulation

The critical superficial air velocity for liquid circulation U_{cl} is the value of superficial air velocity under which liquid begins to circulate between riser and downcomer. Calculated from Eq. (16) where $U_{lr} = 0$, U_{cl} was 1.017 cm min^{-1}, with a concomitant airflow rate of 0.156 L min^{-1}.

To justify U_{cl} model, an experiment was carried out increasing airflow rate gradually from zero and measuring the liquid circulation velocity simultaneously. Fig. 7 shows the results. It was also observed that when $U_{gr} < U_{cl}$, the hydrodynamic behavior of the air and liquid mixture in the riser was similar to that in bubble column and the liquid circulation between riser and downcomer did not exist. However, the mixture circulated upon reaching $U_{gr} > U_{cl}$ and the circulation velocity was

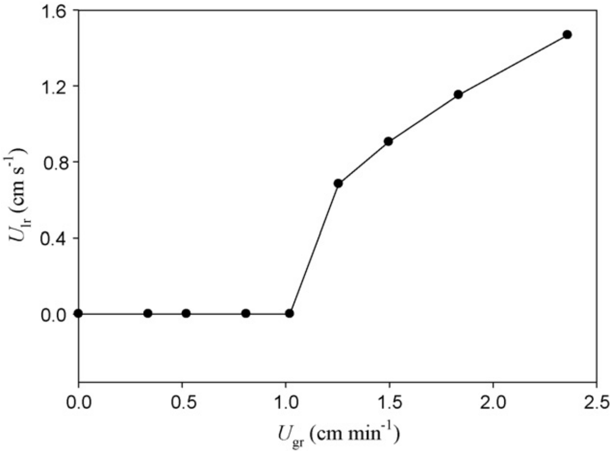

Fig. 7. Results of experiment for verification of critical superficial gas velocity for liquid circulation.

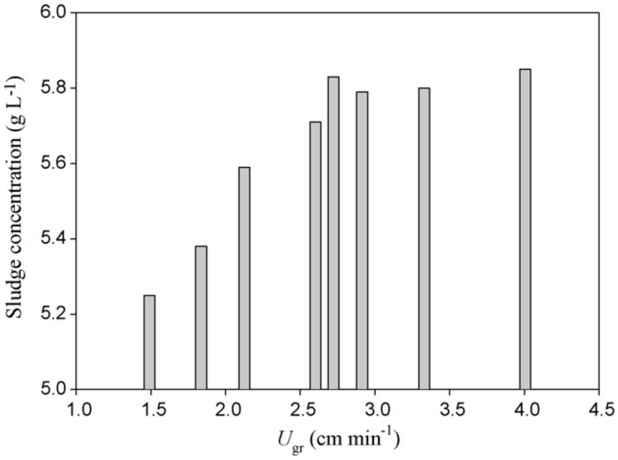

Fig. 8. Variation of average sludge concentration in riser with superficial gas velocity.

obviously enhanced subsequently with an increase in U_{gr}. The experimental results indicated that the model could predict U_{cl} with accuracy.

4.6. *Critical superficial air velocity for granules circulation*

Like U_{cl} for liquid circulation, the critical superficial air velocity for granules circulation U_{cs} is the value of superficial air velocity at which circulation and thorough fluidization of granules begins. Provided that the relationship between U_{gr} and U_{lr} has been established, the critical liquid circulation velocity for thorough fluidization of granules is needed to predict U_{cs}.

Due to the higher sedimentation ability of granular sludge than that of floc-like sludge, the sludge is fluidized completely and circulated in the ALR only when U_{lr} is higher than the highest settling velocity of granules. As mentioned above, the settling velocity was in the range of 0.619–1.550 cm s^{-1}. Therefore, the critical superficial liquid circulation velocity was 1.550 cm s^{-1}. The U_{cs} calculated by Eq. (16) was 2.662 cm min^{-1}, corresponding to an airflow rate of 0.410 L min^{-1}.

An experiment was conducted through determining the sludge concentration in riser at certain U_{gr} to accuracy of the U_{cs} predicted. As the data shown in Fig. 8, when U_{gr} was below the critical predicted value, the sludge concentration was raised with an increase in U_{gr}, indicating that the number of the granules fluidized was enhanced. However, with a U_{gr} higher than the critical value, the sludge concentration, independent of U_{gr}, was kept constant at about 5.80 g L^{-1}. It was suggested that the majority of the granules were fluidized. The experimental results justified the model for prediction of the critical superficial gas velocity for granules circulation.

5. Conclusions

We demonstrated an effective way to develop nitrifying granular sludge by addition of porous solid carriers (activated carbon) within 108 days in continuous-flow airlift bioreactor. Furthermore, a simple and relatively easy to use model is presented to describe the main hydrodynamic parameters in ALR. Gas holdup, liquid circulation velocity, critical superficial gas velocity for liquid circulation, and that for granules circulation can be predicted with accuracy. The gas holdup model developed here was as $\varepsilon_{\mathrm{g}} = 0.942\,U_{\mathrm{gr}}^{0.871}$ and $\varepsilon_{\mathrm{gd}} = 0.732\varepsilon_{\mathrm{gr}} + 0.252$; the liquid circulation velocity model was $U_{\mathrm{lr}} = (2.68 - 0.025\,U_{\mathrm{gr}}^{0.871})\sqrt{0.276U_{\mathrm{gr}}^{0.871} - 0.28}$; the critical superficial gas velocity for liquid circulation and that for granules circulation gained by present investigation was 1.017 and 2.662 cm min^{-1}, respectively.

Acknowledgements

The authors wish to thank the National Hi-Tech Research and Development Program of China (863) (2006AA06Z332), and the Science and Technology Foundation for Key Project of Zhejiang province (2003C13005) for the partial support of this study.

References

[1] G. Lu, P. Zheng, R.C. Jin, M. Qaisar, Control strategy of shortcut nitrification, J. Environ. Sci. 18 (2006) 58–61.

[2] A.F. Ramos, M.A. Gomez, E. Hontoria, J. Gonzalez-Lopez, Biological nitrogen and phenol removal from saline industrial wastewater by submerged fixed-film reactor, J. Hazard. Mater. 142 (2007) 175–183.

[3] R.C. Jin, P. Zheng, Q. Mahmood, B.L. Hu, Osmotic stress on nitrification in an airlift bioreactor, J. Hazard. Mater. 146 (2007) 148–154.

[4] B. Sharma, R.C. Ahlert, Nitrification and nitrogen removal, Water Res. 11 (1977) 897–925.

[5] J. Carrera, I. Jubany, L. Carvallo, R. Chamy, J. Lafuente, Kinetic models for nitrification inhibition by ammonium and nitrite in a suspended and an immobilized biomass systems, Process Biochem. 39 (2004) 1159–1165.

[6] H. Myoga, H. Asano, Y. Nomura, H. Yoshida, Effects of immobilization conditions on the nitrification treatability of entrapped cell reactors using the PVA freezing method, Water Sci. Technol. 23 (1991) 1117–1124.

[7] H. Shan, J.P. Obbard, Ammonia removal from prawn aquaculture water using immobilized nitrifying bacteria, Appl. Microbiol. Biotechnol. 57 (2001) 791–798.

[8] S. Tsuneda, T. Miyoshi, A. Hirata, Biological nitrogen removal of wastewater discharged from demineralizer regenerating process in power plant, Jpn. J. Water Treat. Biol. 37 (2001) 9–17.

[9] Y. Liu, H.L. Xu, S.F. Yang, J.H. Tay, Mechanisms and models for anaerobic granulation in upflow anaerobic sludge blanket reactor, Water Res. 37 (2003) 661–673.

[10] D.S. Shen, X.W. Liu, Y.H. He, Studies on adsorption, desorption and biodegradation of pentachlorophenol by the anaerobic granular sludge in an upflow anaerobic sludge blanket (UASB) reactor, J. Hazard. Mater. 125 (2005) 231–236.

[11] D. Kim, D. Seo, Selective enrichment and granulation of ammonia oxidizers in a sequencing batch airlift reactor, Process Biochem. 41 (2006) 1055–1062.

[12] K.Z. Su, H.Q. Yu, Gas holdup and oxygen transfer in an aerobic granule-based sequencing batch reactor, Biochem. Eng. J. 25 (2005) 201–207.

[13] S. Tsuneda, T. Nagano, T. Hoshino, Y. Ejiri, N. Noda, A. Hirata, Characterization of nitrifying granules produced in an aerobic upflow fluidized bed reactor, Water Res. 37 (2003) 4965–4973.

[14] J.J. Beun, A. Hendriks, M.C.M. van Loosdrecht, E. Morgenroth, P.A. Wilderer, Aerobic granulation in a sequencing batch reactor, Water Res. 33 (1999) 2283–2290.

[15] E. Morgenroth, T. Sherden, M.C.M. van Loosdrecht, J.J. Heijnen, P.A. Wilderer, Aerobic granular sludge in a sequencing batch reactor, Water Res. 31 (1997) 3191–3194.

[16] D. Peng, N. Bernet, J.P. Delgenes, R. Moletta, Aerobic granular sludge—a case report, Water Res. 33 (1999) 890–893.

[17] Y.M. Zheng, H.Q. Yu, G.P. Sheng, Physical and chemical characteristics of granular activated sludge from a sequencing batch airlift reactor, Process Biochem. 40 (2005) 645–650.

[18] R.S. Douek, A.G. Livingston, A.C. Johanson, G.F.I. Hewitt, Hydrodynamic of an external-loop three-phase airlift (TPAL) reactor, Chem. Eng. Sci. 49 (1994) 3719–3737.

[19] P.A. Shamlou, D.J. Pollard, A.P. Ison, M.D. Lilly, Gas holdup and liquid circulation rate in concentric-tube airlift bioreactors, Chem. Eng. Sci. 49 (1994) 303–312.

[20] C. Freitas, J.T. Teixeira, Hydrodynamic studies in an airlift reactor with an enlarged degassing zone, Bioprocess Eng. 18 (1997) 267–279.

[21] Y. Chisti, F. Wenge, M. Moo-Young, Relationship between riser and downcomer gas holdup in internal-loop airlift reactors without gas–liquid separators, Chem. Eng. J. 57 (1995) 7–13.

[22] E. Garcia-Calvo, A. Rodriguez, A. Prados, J. Klein, A fluid dynamic model for three-phase airlift reactors, Chem. Eng. Sci. 54 (1999) 2359–2370.

[23] M. Gavrilescu, R.Z. Tudose, Concentric-tube airlift bioreactors. Part II. Effects of geometry on liquid circulation, Bioprocess Eng. 19 (1998) 103–109.

[24] S.J. Hwang, Y.L. Cheng, Gas holdup and liquid velocity in three-phase internal-loop airlift reactors, Chem. Eng. Sci. 52 (1997) 3949–3960.

[25] B. Kawalec-Pietrenko, Liquid circulation velocity in the inverse fluidized bed airlift reactor, Bioprocess Eng. 23 (2000) 397–402.

[26] Y. Chisti, B. Halard, M. Moo-Young, Liquid circulation in airlift reactors, Chem. Eng. Sci. 43 (1988) 451–457.

[27] Standard Methods for Examination of Water and Wastewater, 19th edn., American Public Health Association/American Water Works Association/Water Environment Federation, New York, 1995.

[28] J. Korpijarvi, Hydrodynamics and mass transfer in an airlift reactor, Chem. Eng. Sci. 54 (1999) 2255–2262.

[29] K.S. Lee, J.F. Wu, Y.S. Lo, Y.C. Lo, P.J. Lin, J.S. Chang, Anaerobic hydrogen production with an efficient carrier-induced granular sludge bed bioreactor, Biotechnol. Bioeng. 87 (2004) 648–657.

[30] A. Ramakrishnan, S.K. Gupta, Anaerobic biogranulation in a hybrid reactor treating phenolic waste, J. Hazard. Mater. 137 (2006) 1488–1495.

[31] M. Green, S. Tarre, M. Schnizer, B. Bogdan, R. Armon, G. Shelef, Groundwater denitrification using an upflow sludge blanket reactor, Water Res. 28 (1994) 631–637.